Prediction of TOA-based localization accuracy using CRLB and 3D buildings with field trial validation

Christophe Villien, Nicolas Deparis, Valérian Mannoni, Sébastien de Rivaz

▶ To cite this version:

HAL Id: hal-03903856

https://hal.science/hal-03903856

Submitted on 16 Dec 2022

Prediction of TOA-Based Localization Accuracy Using CRLB and 3D Buildings with Field Trial Validation

Christophe Villien, Nicolas Deparis, Valérian Mannoni and Sébastien De Rivaz
CEA-Leti, Université Grenoble Alpes, F-38000 Grenoble, France
{christophe.villien, nicolas.deparis, valerian.mannoni, sebastien.derivaz}@cea.fr

Abstract—In Low Power Wide Area (LPWA) networks, radio localization based on Time of Arrival (TOA) measurements collected from gateways synchronized on GPS time is an appealing technology for Internet of Things (IoT). However, it is hard to predict the actual accuracy that could be expected from a given deployment without taking into account the propagation channel complexity. This paper proposes a new approach to generate a localization accuracy map (LAM) based on Cramér-Rao lower bound (CRLB) and 3D buildings models to predict the propagation conditions. A comparison with measurements from LPWA field trials conducted in the city of Grenoble (France) is presented, comprising more than 300 000 LPWA transmissions collected. We show that for an infrastructure composed of 6 LPWA gateways, our LAM is able to predict the performance obtained with an maximum likelihood estimator (MLE) localization algorithm with only 12% of mismatch.

Keywords—Low Power Wide Area Network (LPWAN); LoRa; LoRaWAN; Path Loss; Measurement; Urban propagation; TDOA; Localization; Accuracy; Field Test

I. INTRODUCTION

The Internet of Things is playing a major role across a variety of vertical applications, generating cost savings, new revenue streams and other benefits. Among the possible Internet of Things (IoT) connectivity technologies, new approaches referred as Low Power Wide Area (LPWA) networking have emerged. These technologies give a low power connectivity alternative while covering large areas with a narrow bandwidth. The main LPWA communication systems are: Narrowband IoT (NB-IoT) derived from the 3GPP LTE, operating in a 180 KHz bandwidth, and the proprietary solution Semtech Long Range (LoRaWAN), operating in a 125 KHz bandwidth. These LPWA systems present quite similar Maximum Coupling Loss (MCL > 164 dB) and may both operate in same frequency range (800-900 MHz) in Europe.

Remote monitoring and wearable technologies could help to effectively manage health, monitor safety and reduce the staggering healthcare costs. In this use case, currently under study by the H2020 Project 5G-HEART [1], a vital sign patch is used to monitor the patients remotely and to trigger an emergency alert when patients suffering from critical conditions require immediate help. Strong requirements to localize the patient are then put on the patch for emergency services to effectively assign resources at the right location. This wearable vital-sign patch must be low complexity (cost), small size and requires a long battery life. This means that the connectivity used for uploading patient vital-signs is based on LPWA technology and also that geo-location should be realized with minimal energy-expenditure and minimal additional hardware. For those reasons using an GNSS receiver is not an option,

adding to the fact that indoor coverage of those technologies is virtually non-existent. Therefore, the focus should be on using the existing LPWA radio technology, as well through gateway multilateration.

One challenge for localization systems is to optimize the network infrastructure (e.g. gateways position, PHY radio parameters) to get the highest location accuracy. In other words, the challenge is to be able to predict location precision taking into account both propagation environment and gateways position with dedicated models. The accuracy is usually computed through the CRLB considering various metrics such as TOA [2] [3], time-difference-of-arrival (TDOA) [4], angle-of-arrival (AoA) or fusion of several metrics [5]. However, few authors address the influence of hybrid propagation that mixes line-of-sight (LOS) and non-line-of-sight (NLOS) channels [3], and it is seldom that computed bounds are tested against real measurements or only with limited datasets and scenarios [6]. Large scale field tests using LPWA (SigFox, LoRaWAN) real measurements including both LOS/NLOS propagation has already been conducted [7] , but it has not been used to build accuracy models.

In this study, we consider the prediction of a localization accuracy map (LAM) based on CRLB computation for TOA measurements, while addressing the hybrid LOS/NLOS propagation channel using 3D building models. Moreover, a LPWA network of 6 gateways with accurate TOA measurements capability has been deployed and a large database comprising more than 300 000 LPWA transmissions has been build in order to asses the quality of the LAM by comparison with a localization algorithm based on maximum likelihood estimation (MLE).

This paper is then structured as follows. After introducing the theoretical background of CRLB and MLE in section II, the field trial setup is described in section III. Implementation of the LAM generation and measurements processing is provided in section IV. Finally, performance of our prediction models are detailed in section V and the synthesis is given in the conclusion in section VI.

II. PROBLEM STATEMENT

In this study, we aim at analyzing the location accuracy based on TOA measurements by computing some performance bound for each position $\mathbf{r}_k = [x_k, y_k, z_k]^T$ belonging to a set of n positions arbitrarily defined, $\mathbf{r}_k \in M = \{\mathbf{r}_1, \mathbf{r}_2, \ldots, \mathbf{r}_n\}$ which we call LAM.

A. Measurement model

If we consider a single transmission from a position $\mathbf{r}_k$ to a gateway with coordinates $\mathbf{r}_g = [x_g, y_g, z_g]^T$, the pseudo range

$\rho_{g,k}$ (i.e. TOA multiplied by the speed of light c) measured by the gateway g can be modelled as

$$\rho_{g,k} = h_g(\mathbf{r_k}, d_0) + \mu_g(\mathbf{r_k}) \tag{1}$$

where h_g is the measurement function associated to gateway g defined by

$$h_g(\mathbf{r}_k, d_0) = \sqrt{(x_k - x_g)^2 + (y_k - y_g)^2 + (z_k - z_g)^2} + d_0 \tag{2}$$

where $d_0 = c \cdot t_0$ is the distance offset, with t_0 the unknown departure time of the signal and $\mu_g(\mathbf{r_k})$ a Gaussian distributed random variable that represents all the errors of the measurement process, including gateway related errors (e.g. synchronisation errors, time of arrival detection uncertainty) but also channel errors due to multipath and NLOS propagation. Although channel is essentially static and thus, channel errors are highly correlated over time (i.e. channel errors are biased), here we are considering their spatial distribution that we assume to be independent from one position to another (i.e. $\mathbb{E}[\rho_{k,g}\rho_{j,g}] = 0$ for $j \neq k$). In the general case, we shall assume that the error distribution is different for every considered position $\mathbf{r}_k$ because propagation conditions vary which makes the accuracy difficult to predict. In this study, we will assume that the TOA error distribution measured by a gateway g when transmitter is located at position $\mathbf{r}_k$ depends only on the channel conditions between these two points :

$$\mu_g(\mathbf{r_k}) \sim \begin{cases} \mathcal{N}(0, \sigma_{LOS}^2) & \text{if } \delta_{LOS}(\mathbf{r}_k, \mathbf{r}_g) = 1 \\ \mathcal{N}(0, \sigma_{NLOS}^2) & \text{if } \delta_{LOS}(\mathbf{r}_k, \mathbf{r}_g) = 0 \end{cases} \tag{3}$$

with $\delta_{LOS}(\mathbf{r}_k, \mathbf{r}_g)$ a function that is equal to 1 if the position $\mathbf{r}_k$ and $\mathbf{r}_g$ are in LOS, and 0 otherwise. Motivations for distinguishing between these two cases are that, in NLOS situations, the direct path of the radio wave can be blocked (e.g. by a building) and only reflected signals are received by the gateway. Because reflected signals travels longer distances than the direct path, the effective time-of-flight (TOF[1]) experiences an excess delay resulting in a stronger TOA error than for direct propagation.

B. Position estimation using TOA measurements

Localization based on TOA measurements requires that all receiving gateways are synchronized which is achieved thanks to GPS signal (see sec. III). However, such a synchronization cannot be assumed for the mobile tag whose departure time t_0, or equivalently $d_0 = c.t_0$, is unknown and must be estimated in addition to the position. Because most LPWA networks use low duty-cycles transmissions (e.g. 1 uplink packet over several minutes or hours) not much information can be obtained from previous location estimations in case of mobility, hence single epoch processing (i.e. based on a single transmission) is well suited for such applications. Assuming that the height (i.e. $_k$) of the transmitter is known with an accuracy of a few meters, the problem turns out to a parameter estimation

$$\mathbf{x}_k = [x_k, y_k, d_0]^T \tag{4}$$

subject to the measurements

$$\rho_k = [\rho_{1,k} \quad \rho_{2,k} \quad \cdots \quad \rho_{n,k}]^T \tag{5}$$

which are distributed according to

$$\rho_k \sim \mathcal{N}(\mathbf{h}(\mathbf{x}_k)), \mathbf{R}_k) \tag{6}$$

---

[1]Here TOF refers to the propagation time, contrary to the TOA which refers to the actual time of reception, time of departure being unknown

with $\mathbf{h}(\mathbf{x_k}) = [h_1 \quad h_2 \quad \cdots \quad h_n]^T$ the vector of the measurement functions and $\mathbf{R}_k$ the covariance matrix of the measurements which we assumed to be independent $(\mathbf{R}_k)_{i \neq j} = 0$. We also assume that their variances, expressed by the diagonal coefficients $(\mathbf{R}_k)_{i,i} \in \{\sigma_{LOS}^2, \sigma_{NLOS}^2\}$, depend on the channel conditions between the gateway g and the position $\mathbf{r}_k$ according to our model in Eq. (3). The parameter $\mathbf{x}_k$ can be estimated using a MLE given by

$$\hat{\mathbf{x}}_k = \arg \max_{\mathbf{x}_k} \ln l(\rho_k, \mathbf{x}_k) \tag{7}$$

where $\ln l(\rho_k, \mathbf{x})$ is the logarithm of the likelihood function associated to the measurements distribution, which are in our case of normaly distributed, and is expressed as

$$\ln l(\rho_k, \mathbf{x}_k) = -\frac{1}{2} \Big[\ln |\mathbf{R}_k| + n \ln(2\pi) + \dots$$
$$(\rho_k - \mathbf{h}(\mathbf{x}_k))^T \mathbf{R}_k^{-1} (\rho_k - \mathbf{h}(\mathbf{x}_k)) \Big] \tag{8}$$

where $|\mathbf{R}_k|$ is the determinant of the matrix $\mathbf{R}_k$. One sees easily that maximizing Eq. (8) is equivalent to minimizing

$$\hat{\mathbf{x}}_k = \arg \min_{\mathbf{x}_k} \big((\rho_k - \mathbf{h}(\mathbf{x}_k))^T \mathbf{R}_k^{-1} (\rho_k - \mathbf{h}(\mathbf{x}_k)) \big) \tag{9}$$

In practice, the solution of the Eq. (9) can be computed using an optimization algorithm (e.g. Leveberg-Marquardt, Steepest Descent [8], etc.).

When the position $\mathbf{r}_k$ is known and only the distance offset d_0 should be estimated (i.e. to compute TOA error for a given gateway), Eq. (9) simplifies and the estimated solution is given by the weighted sum

$$\hat{d}_0 = \frac{1}{s_\omega} \sum_{g=1}^{n} \omega_g (\rho_{g,k} - d_{g,k}) \tag{10}$$

with $d_{g,k}$ the (known) distance between the gateway g and the considered position $\mathbf{r}_k$, the weight $\omega_g = 1/(\mathbf{R}_k)_{g,g}$ and $s_\omega = \sum_{g=1}^{n} \omega_g$ the normalization coefficient.

C. Cramér-Rao lower bound

The location accuracy on a given point $\mathbf{r}_k$ of a map M will depend on the geometry of the deployment (i.e. position of each gateway w.r.t. to this point), the accuracy of each TOA measurement described by the distribution of $\mu_g(\mathbf{r}_k)$ and the efficiency of the algorithm used to compute the estimated location. Although the former two aspects have been modeled, it is very hard to describe the performance of an algorithm in the general case. A workaround to this problem is to compute the best achievable accuracy (i.e. instead of the actual accuracy), which cannot be beaten by any algorithm in a statistical sense and under certain conditions. The well-known Cramér-Rao lower Bound (CRLB) [4] provides such a lower bound for any unbiased estimator, and states that

$$\mathbb{E}[(\hat{\mathbf{x}}_k - \mathbf{x})(\hat{\mathbf{x}}_k - \mathbf{x})^T] \geq \mathbf{J}_k^{-1} \tag{11}$$

with $\mathbf{J}_k$ the Fisher information matrix (FIM) defined as

$$\mathbf{J}_k = \mathbb{E}[\nabla_\mathbf{x} \ln l(\rho_k, \mathbf{x})(\nabla_\mathbf{x} \ln l(\rho_k, \mathbf{x}))^T] \tag{12}$$

with $\ln l(\rho_k, \mathbf{x})$ the log-likelihood given in Eq. (8). Taking the gradient descent and noting that

$$\mathbb{E}[(\rho_k - \mathbf{h}(\mathbf{x}_k))(\rho_k - \mathbf{h}(\mathbf{x}_k))^T]\mathbf{R}_k^{-1} = \mathbf{I_3} \tag{13}$$

we obtain the following expression (Cf [4])

$$\mathbf{J_k} = \nabla_{\mathbf{x}}\mathbf{h}.\mathbf{R}_k^{-1}.\nabla_{\mathbf{x}}\mathbf{h}^T \qquad (14)$$

where

$$\nabla_{\mathbf{x}}\mathbf{h} = \begin{bmatrix} \frac{x_k-x_1}{\|\mathbf{r}_k-\mathbf{r}_1\|} & \frac{x_k-x_2}{\|\mathbf{r}_k-\mathbf{r}_2\|} & \cdots & \frac{x_k-x_n}{\|\mathbf{r}_k-\mathbf{r}_n\|} \\ \frac{y_k-y_1}{\|\mathbf{r}_k-\mathbf{r}_1\|} & \frac{y_k-y_2}{\|\mathbf{r}_k-\mathbf{r}_2\|} & \cdots & \frac{y_k-y_n}{\|\mathbf{r}_k-\mathbf{r}_n\|} \\ 1 & 1 & \cdots & 1 \end{bmatrix} \qquad (15)$$

and $\|.\|$ denotes the norm operator. It should be noted that the FIM $\mathbf{J_k}$, and consequently the accuracy bound, depends on the considered position $\mathbf{r}_k$ on the map M, the gateway position $\mathbf{r}_g$, the channel condition between these two points and finally both parameters σ_{LOS} and σ_{NLOS} that should be determined.

III. DESCRIPTION SYSTEM SETUP

A. Gateway Characterization

In order to perform precise and accurate TOA measurements, COTS telecom grade gateways iBTS from manufacturer Kerlink (see Fig. 3) based on the LoRaWAN technology have been considered. These gateways have fine time-stamping capability, and are synchronized with the GPS time through a Pulse-per-Second (PPS) signal generated by GNSS receiver included in the gateway with an accuracy of a few nanoseconds.

According to LoRaWAN specifications [9], the *DR* (DataRate) parameter can be tuned to optimize the trade-off between data rate (high data rate *DR*=5 / MCL=144 dB) and coverage (low data rate *DR*=0 / MCL=164 dB). This parameter controls the LoRa physical layer and has a strong impact on the gateway performance. The laboratory setup used to perform TOA characterization for different values of *DR* versus RSS (Received Signal Strength) is detailed bellow.

A GNSS emulator is configured to send through a RF cable a GNSS static radio signal to two iBTS gateways: g_A and g_B. A LoRaWAN device, which *DR* value can be controlled by software, is configured to continuously send packets to these two gateways with identical RF cables and so same propagation distances d_A and d_B.

We consider the TDOA between the two gateways from a received packet defined as

$$\delta t_{AB} = \rho_{g_A} - \rho_{g_B} \qquad (16)$$

From Eq. (1) and Eq. (16) and because the propagation distances d_A and d_B are identical, TDOA can be expressed as

$$\delta t_{AB} = 2\mu_g(RSS) \qquad (17)$$

Taking advantage of a conducted propagation, we assume that TOA errors follow a specific law that is only RSS dependent[2].

$$\mu_g(RSS) \sim \mathcal{N}(0, \sigma_{TOA}^2(RSS)) \qquad (18)$$

An adjustable RF attenuator is used to control the power received by these gateways, and a dedicated software enables to store in a database the TOA, RSS and signal-to-noise (SNR) radio metrics for each gateway according to the different LoRaWAN device uplink *DR* values.

A first calibration is performed to insure that both gateways measure the same RSS and SNR for all the attenuation values. The TDOA values for DR=5 is plotted in Fig. 1 as the function
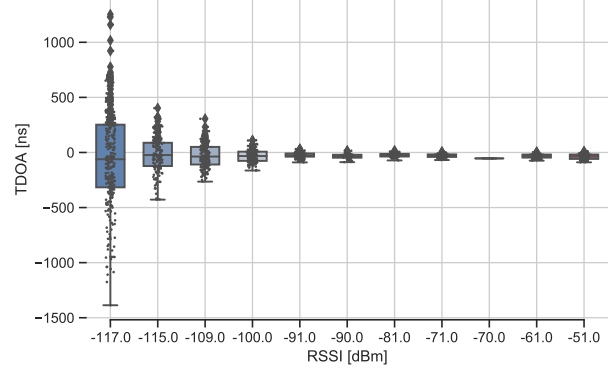

Fig. 1. TDOA values versus RSS for DR=5

of RSS. One may notice that for high RSS values (i.e. RSS >-100 dBm), the σ_{TDOA} (with $\sigma_{TDOA} = \sqrt{2}\sigma_{TOA}$) is lower than 20 ns which compares with a typical GNSS PPS jitter value. For lower values RSS values (RSS <-115 dBm), σ_{TDOA} increases from 300 ns up to a little bit more than $1\mu s$, which represents an error distance of more than 300 meters. The standard deviation σ_{TDOA} for all possible DR values is shown in Fig. 2. As expected, we note that the accuracy of TDOA is better for lower data rates.
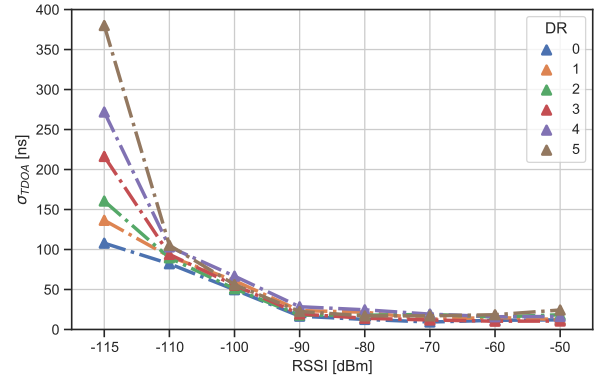

Fig. 2. TDOA standard deviation versus RSS for different DR Values

B. Network Infrastructure

The infrastructure is composed of 6 iBTS gateways as described in section III-A. Because some sites of implantation were not available at the beginning of the data collection process, three gateways (i.e #4, #5 and #6, see in Table I), have been temporarily installed on the roof of one building in CEA premises, and thus were located at the same position which is also very close (i.e. about 50m) from gateway #1, resulting in a subset of 4 gateways with very poor geometric dilution of precision (GDOP). At the very end of the measurement campaign they have been moved to their final locations (i.e. #7, #8 and #9). Taking advantage of the fact the city of Grenoble is surrounded by mountains, some gateways have been installed on very high spots, especially gateways #2 and #3 which are both installed on the roof of cable car arrival stations at

---

[2]for the sake of clarity, the dependence to RSS will be omitted.

altitudes of 485m (Fig. 3) and 2259m respectively, offering a very wide radio coverage, even if this latter is located at more than 15km from the city.

A tenth of LoRaWAN LPWA devices, embedding a GNSS receiver which is used to provide a reference position, have been distributed to volunteers to collect their locations via an uplink packet, during their daily trips over a period of a little bit more than one year. These trips include mainly car, bicycle and pedestrian displacements. The LoRaWAN network topology is star-of-stars, in other words, each device uplink packet can be received by more than one gateway, mainly depending on path loss attenuation and local interference. A LoRaWAN Network Server (LNS) is used to collect information from gateways. The CEA infrastructure network, including its LNS, is used to store in a database for post-processing various metrics, such as, but not limited to : i. device extended unique identifier (EUI) ii. gateways radio metrics : TOA, RSS SNR iii. uplink network parameters : frequency, DR.

Over the test campaign period (which is still going on at the time of writing this paper), a total of 323453 uplink packets have been recorded into the database, which is nearly 3 times more than comparable studies [7]. We can see in Table I that the number of packets actually received is very different for each gateway, which is mainly explained by their activity period. In particular, the gateways #7 and #8 have been installed very recently and have been collecting packets for only two weeks, whereas the installation of gateway #9 is still in progress. The best efficiency of 72% is achieved by the gateway #2 thanks to its very favourable location overhanging the city of Grenoble as illustrated in Fig. 3.

Fig. 3. Gateway installed on the roof of the cable-car arrival station at Bastille, overhanging the city of Grenoble, France.

TABLE I.   DEPLOYMENT CHARACTERISTICS

#	Name	Location	Altitude	Duration	#packets
1	BCC@CEA	[-127m, -53m]	250m	13 months	233399
2	Bastille	[1262m, 485m]	493m	13 months	230909
3	Chamrousse	[15278m, -7601m]	2259m	13 months	184529
4	B2I-test$_A$ @CEA	[-60m, 65m]	236m	13 months	187970
5	B2I-test$_B$ @CEA	[-60m, 65m]	236m	2 months	25555
6	B2I-test$_C$ @CEA	[-60m, 65m]	236m	2 months	18766
7	Pont-De-Claix	[-872m, -8145m]	291m	2 weeks	678
8	Vouillants	[2686m, -2198m]	559m	2 weeks	1171
9	Alpexpo	[2063m, -4294m]	232m	0 weeks	0

IV.   PROCESSING IMPLEMENTATION

A. Map model and map matching

The map M has been constructed on a grid of 10m×10m cells over a square area of 40km× 40km centered on site of CEA which is located close from downtown. Hence, the map represents a potential of 16 million of cells, but only those who actually collect at least one measurement are fully initialized, which represent a total of about 40 000 cells after 13 month of data collection. Because the LPWA embedded GNSS receiver present position accuracy that can be worst than the cell size especially in urban environment, a map matching is performed before assigning a packet to a cell. This operation uses the road network from Open Street Map (OSM) database by pre-allocating any cell whose location matches certain type of "ways" (i.e. according to OSM representation) including the streets, highways, hiking trails etc. When a new packet is received, it will be assigned to the closest pre-allocated cell in a range of 50m w.r.t. to GNSS position and, if no cell is found, it will be assigned to the closest cell of the grid.

B. LOS analysis using 3D buildings map

One central aspect of this study is to evaluate the benefits of prior knowledge about channel conditions between the transmitter and the receiver. Hence, for each cell, this information will be computed with respect to each gateways using a ray-tracing tool included in Matlab Communication Toolbox©, which provides a binary information (LOS or NLOS) by detecting if the segment connecting two points intersect any building from the loaded OSM buildings map as illustrated on Fig. 4. Because this operation is computationally intensive, the full map is split into several "LOS Analysis Area" (LAA) of 2km×2km (with 500m of overlap between two adjacent LAA to avoid processing points on the LAA borders), and only buildings belonging to the considered LAA are loaded for processing. Using this technique, it reduces the processing time to approximately 10s per cell for computing all gateways visibility conditions and also predict the RSS from a propagation model although this is not used in this study.

Fig. 4. Overview of LOS analysis

C. Cell structure and processing

Each cell gathers different types of information among which i. static properties such as its position in a local frame of reference and channel conditions with respect to each gateway but also the "full" CRLB corresponding to the accuracy for a packet received by all gateways, ii. all measurements (e.g TOA, RSS etc.) assigned to the cell, iii. results of cell computations which includes measurement statistics (mean value, standard deviations, etc.), various CRLB and MLE results (see algorithm 1).

It should be noted that several configurations exist for a given cell, depending on the number of gateways receiving each packet. Indeed, some gateways will never received a packet transmitted from a certain location because the pathloss is to strong, but it may also happen that an interferer prevent a packet of being received even-though the signal power is above the gateway sensitivity. For this reason, if a cell k receives p_k packets, all results (MLE locations and location errors, CRLB, etc.) are computed independently for each packet and denoted as $v^{(i)}$, the computed value v from packet #i. Only the results corresponding to the best configuration are retained for analysis, where the best configuration is defined as the one that minimize the CRLB, which can also be interpreted as the best GDOP.

Algorithm 1 Cell k processing

1: **for** all received packets $i \in \{1, 2, \ldots, p_k\}$ **do**
2:      Select valid measurements $\rho_{\mathbf{k}}^{(i)}$
3:      Estimate $\hat{d}_0^{(i)}$ using Eq. (10)
4:      Compute TOF error $\delta\rho_k^{(i)} = \rho_k^{(i)} - (\mathbf{d}_k - \hat{d}_0)$
5:      Compute Full solution $\hat{\mathbf{x}}_k^{(i)}$ using Eq. (9)
6:      Compute position error $\delta\mathbf{x}_k^{(i)} = \hat{\mathbf{x}}_k^{(i)} - \mathbf{x}_k$
7:      Compute CRLB $\mathbf{J}_k^{-1(i)}$ using Eq. (12)
8: **end for**
9: Select best configuration : $i_{best} = \arg\min_i \left\| \mathbf{J}_k^{-1(i)} \right\|$
10: Record best values: $\mathbf{J}_k^{-1(i_{best})}, \delta\mathbf{x}_k^{(i_{best})}$
11: Compute TOF statistics (mean, std, rms, etc.)

V. RESULTS

A. TOA distribution

Besides the map preparation which includes the computation of channel conditions for each cell with all gateways, two important parameters are required by the model for the LAM prediction and localization algorithm which are σ_{LOS} and σ_{NLOS} (see Eq. (3)). Lab measurements (Cf section III-A) give a first idea of the value σ_{LOS} in an ideal case of conducted propagation. However, real propagation is much more complex, mainly because of multipath and signal obstruction. Hence, empirical cumulative distribution functions (CDF) of TOA errors have been computed as described in algorithm 1, and the most relevant ones (i.e. based on a sufficient number of values) have been plotted according to their channel conditions as shown in Fig. 5. Interestingly, these CDF show that the two gateways (#2 and #3) with high altitudes (>500m) are insensitive to their channel conditions as their LOS and NLOS curves nearly overlap, both having a P68 metric (i.e. 68% of the samples below the P68 value) equal to approx. 250m. One possible explanation is that the high elevation gateways (i.e. elevation angle is a more relevant indication than altitude

in that context), if not in LOS, are most often in near-LOS situation which is not detected by Matlab ray-tracing tool. Indeed, it can be assumed that in a NLOS condition a portion of the radio wave can reach the top of surroundings buildings by reflection with short extra path length, and from that point, the radio wave can reach a high elevation gateway with LOS conditions. The same reasoning is not true for low elevation gateways because some additional obstacles (e.g. buildings) can be found on the wave path which propagates horizontally.

Another important result that can be highlighted from these CDF illustrated in Fig. 5, at least for the low elevation gateways (i.e. #1 and #4), is the ability to predict the TOA accuracy using the 3D map information of the buildings. We clearly see that CDF of TOA errors is significantly degraded (P68=710m and P68=1300m) for cells predicted as NLOS compared to cells predicted as LOS (390m and 380m for gateways #1 and #4 respectively), which validates the approach. Nonetheless, we observe a difference for the σ_{LOS} values between high and low elevation gateways (i.e. 250m and 380m respectively) which is not fully understood but which probably originates from higher multipath level in case of low elevation gateways.

It should also be noticed that the TOA accuracy is significantly degraded in real conditions even in LOS conditions (i.e. 250m and 380m) with respect to conducted propagation where the jitter (100ns for DR0 mode, see section III-A) would corresponds to 33m of TDOA errors, that is to say 23m of TOA error.

B. LAM prediction

In a first step, the LAM has been generated using $\sigma_{LOS} = 230m$ and $\sigma_{NLOS} = 1000m$ according to their empirical distributions (Fig. 5), and compared to the actual errors of the estimated locations from MLE (using same parameters) to assess the prediction quality of the model. Restrictively, because 3 sites were not available during most of the measurement campaign (see in Table I), 4 gateways out of 6 were installed at the same place (i.e. "CEA") resulting in a poor GDOP. Hence, cells corresponding to a very large GDOP (i.e. received by an insufficient number of gateways < 3 or only by gateways located at CEA) have been discarded, resulting in a total of 8835 cells valid for comparison. For each of those cells, the location and the CRLB corresponding to the best configuration have been computed as explained in section IV-C. Fig. 6 compares the CDF empirical distribution
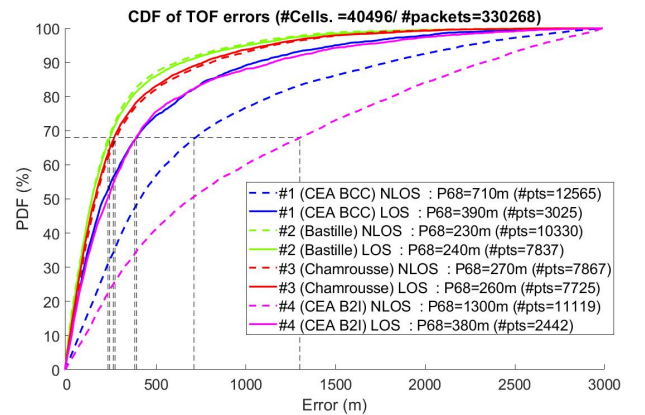

Fig. 5.   TOA errors empirical CDF for different gateways according to their channel conditions

of the MLE positioning errors and its prediction from CRLB for cells belonging to an arbitrary defined "analysis zone" of 5.5km×5.5km, for which the predicted errors are reasonably low (see Fig. 7). We see that the expected errors are quite large with a P68 metric of about 3km because of the poor GDOP as explained before. Nonetheless, we see a very good match between the CRLB and the MLE errors with only 12% of difference regarding the P68 metric and very similar CDF, which is the main purpose of this study. We also note that the CDF of the position errors are slightly better than the CRLB, which indicates that the chosen parameters (i.e. $\sigma_{LOS/NLOS}$) of our model are little too pessimistic with respect to reality.

Then, the accuracy map has been computed for the full gateway set in Table I. Accuracy prediction has been computed only for initialized cells (i.e. containing one measurement at least), resulting in the map shown in Fig. 7. As expected, the convex hull formed by the gateways corresponds to the best accuracy area, whereas the precision degrades out of this zone. According to this map, the positioning error should not exceed 300m in the analysis zone which can be verified as the data collection goes on.

VI. Conclusion

In this paper we have studied the feasibility of LAM prediction based on TOA measurements by using 3D buildings map and CRLB computation. Our model assumes different TOA distributions according to the channel conditions of each considered gateway-cell pair. The quality of this prediction has been assessed by comparison with a MLE-based location algorithm applied on a large data set of real measurements, and by analysis of TOA errors in conducted propagation as well as in radiated propagation conditions. This analysis clearly shows different distributions (i.e. $\sigma_{LOS} = 230m$ vs $\sigma_{NLOS} = 1000m$) for low elevation gateway according to their channel conditions with the considered point. One of the other notable results is the demonstration of a certain immunity to the effect of NLOS channels on TOA accuracy for gateways having high elevation, which seems to be always in LOS or in a near-LOS situation. This is not detected by Matlab© LOS detection function which only returns a binary information about the presence or not of an obstacle, but we believe that our approach would benefit from a slightly richer information about the channel conditions, like the depth of the obstacles on the way of the direct
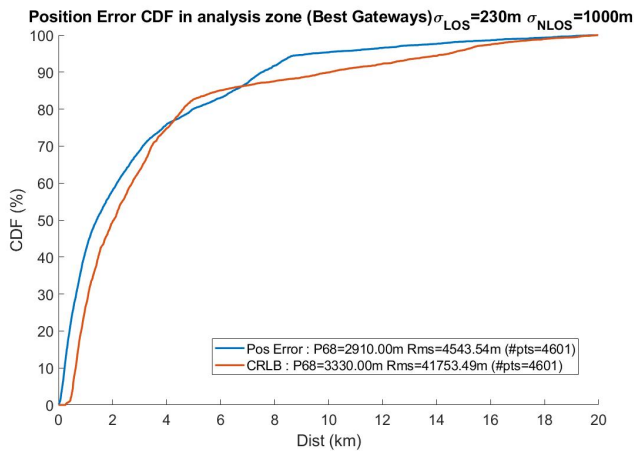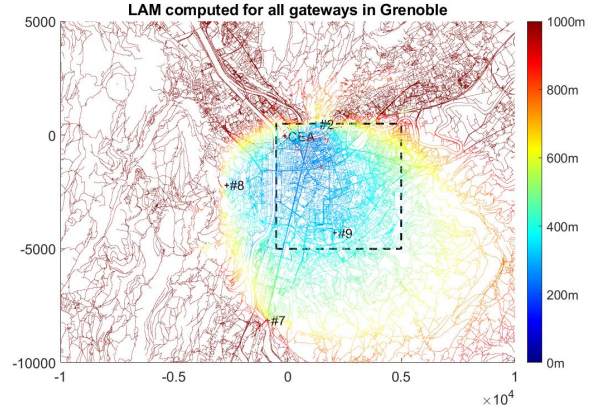

Fig. 7. LAM for Grenoble city area

path. A first LAM has been generated according to the TOA error models found and the gateways position used during the data collection. This LAM has then been compared to the actual errors obtained from a MLE-based location algorithm, showing a very good match between the two (e.g. only 12 % of difference for the P68 in the analysis zone). Location errors are significantly higher (e.g. P68=3000m) than those usually reported in the literature but this is mainly explained by the poor GDOP of the initial gateway deployment and perfectly predicted by our model (P68=3300m). According to the same model, the accuracy of the new deployment should be close to 300m in the same zone, which can be verified as the measurement campaign is still going on.

References

[1] P. H. Lehne et al., "D3.1: Healthcare Vertical Trial Requirements Definition and Execution," Tech. Rep., 5GHEART deliverable Tech. Rep, October 2019.

[2] T. Jia and R. M. Buehrer, "A new cramer-rao lower bound for toa-based localization," in *MILCOM 2008 - 2008 IEEE Military Communications Conference*, 2008, pp. 1–5.

[3] Y. Zhao et al., "Er-crlb: An extended recursive cramér–rao lower bound fundamental analysis method for indoor localization systems," *IEEE Trans. on Vehicular Technology*, vol. 66, no. 2, pp. 1605–1618, 2017.

[4] R. Kaune, "Accuracy studies for tdoa and toa localization," in *2012 15th International Conference on Information Fusion*, 2012, pp. 408–415.

[5] Y.-Y. Li, G.-Q. Qi, and A.-D. Sheng, "Performance metric on the best achievable accuracy for hybrid toa/aoa target localization," *IEEE Communications Letters*, vol. 22, no. 7, pp. 1474–1477, 2018.

[6] C. Xu et al., "Toward near-ground localization: Modeling and applications for toa ranging error," *IEEE Trans. on Antennas and Propagation*, vol. 65, no. 10, pp. 5658–5662, 2017.

[7] M. Aernouts, R. Berkvens, K. Van Vlaenderen, and M. Weyn, "Sigfox and lorawan datasets for fingerprint localization in large urban and rural areas," *Data*, vol. 3, no. 2, 2018.

[8] T. K. Moon and W. C. Stirling, *Mathematical Methods and Algorithms for Signal Processing*. Prentice Hall, 2000.

[9] "LoRaWAN Specification v1.1." [Online]. Available: https://lora-alliance.org/resource_hub/lorawan-specification-v1-1/

Fig. 6. Position CDF and CRLB horizontal errors in the best configuration